Dendrimer-Tetrachloroplatinate Precursor Interactions. 2. Noncovalent Binding in PAMAM Outer Pockets

Francisco Tarazona-Vasquez and Perla B. Balbuena*

Department of Chemical Engineering, Texas A&M University, College Station, Texas 77843

Received: August 3, 2006; In Final Form: December 14, 2006

Density functional theory is used to investigate the complexation ability of dendrimer outer pockets—in both tertiary amine protonated and unprotonated scenarios—toward molecular guests, particularly tetrachloroplatinate-(II) and its mono- and diaquated derivatives as well as competing counterions. The effect of the outer pocket (host) on the binding affinity of guest molecules is analyzed and it is found that is more feasible for the host to accept species, particularly charged ones, inside an unprotonated pocket rather than outside; unlike the protonated pocket where the opposite is more likely to occur. Conformational changes triggered by the hosting of particular guests can have an impact in the global configuration of the larger dendrimer the pockets are part of.

1. Introduction

Metal nanoparticles are increasingly sought for applications in electronics[1] and catalysis.[2] Among a variety of fabrication methods,[3] nanoparticles are synthesized from chemical precursors via complexation inside of macromolecular templates and posterior reduction.[4] However, present challenges in such nanoparticle fabrication methods merit further investigations on the prereduction stages such as ionic complexation particularly in poly(amino amide) (PAMAM) dendrimers.

Platinum nanoparticles can be obtained by reducing tetrachloroplatinate anions; the potassium salt is commonly used as a precursor.[5−8] Concentrations as high as 0.04−0.09 M[9] and as low as 10 μM[10] have been used in characterization of binding of $PtCl_4^{2-}$ to dendrimers. Typical concentrations for nanoparticle synthesis are in the midconcentration range (0.001−0.003 M).[8,11]

As soon as a precursor salt is dissolved, aquation or hydrolysis of $PtCl_4^{2-}$ proceeds with displacement of chloride ligands by water solvent molecules. Because the first hydrolysis step is proportional to the concentration of $PtCl_4^{2-}$,[12] the larger the concentration of precursor salt, the faster aquation takes place until thermodynamic equilibrium is reached. pH will determine which species are present.[12,13]

The distribution of tetrachloroplatinate anion and its mono- and diaquated species at equilibrium conditions is calculated as a function of the initial concentration of precursor salt with the equilibrium constants assigned for the first and second hydrolysis[14] and is used to compute the percentage of abundance of these species shown in Figure 1. For instance, a completely equilibrated solution of 0.09 M (the concentration used in NMR experiments with G2OH)[9] should contain 68% $PtCl_4^{2-}$, 31% $PtCl_3(H_2O)^-$ and 1% $PtCl_2(H_2O)_2$.

Because $PtCl_3(H_2O)^-$ was detected by NMR measurements,[9] it is important to study the interactions of dendrimer pockets not only with $PtCl_4^{2-}$ but also with its mono- and diaquated species. Such study can provide insight on the complexation ability of dendrimer pockets for steadily hosting low charged species.

* To whom correspondence should be addressed. E-mail: balbuena@tamu.edu.

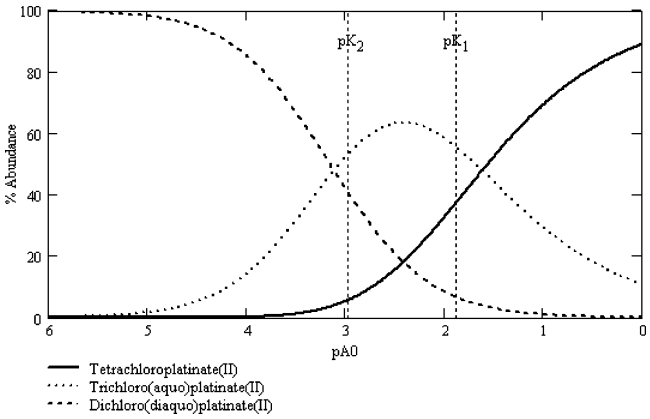

Figure 1. Percent of abundance at equilibrium (aged) conditions of tetrachloroplatinate ($PtCl_4^{2-}$) and its mono- and diaquated species as a function of initial concentration of precursor salt K_2PtCl_4 (pA0). At high initial concentration the tetrachloroplatinate anion is predominant whereas the diaquated is the predominant species at low concentration in its cis and trans isomeric forms.[15] At medium concentration (about 0.01−0.001 M) the predominant species is the monoaquated one. A percentage of abundance for each species is defined as [species A] × 100/[total]; constants K_1 and K_2 are given by Cotton and Wilkinson;[14] "pA0" in the abscissa axis is defined as $pA_0^{2-} = -\log([K_2PtCl_4]_0)$.

Metal precursor binding can also be affected not only by pH[16] but also by competing species present in solution,[17] like counterions K^+ and Cl^-. By studying these interactions and how they relate to each other, we expect to obtain a better understanding of the complexation process itself.

In this paper we analyze the binding affinity of the metal precursor tetrachloroplatinate(II) and its mono- and diaquated species for water dimer and monohydrated hydronium and for a water dimer hosted inside unprotonated and protonated PAMAM-OH outer pockets. The relative strength of these interactions will enable us to establish the feasibility of a given reaction toward guest hosting.

2. Models and Computational Procedures

At least in the early stages of precursor−dendrimer interaction and before reaching the inner voids, precursor molecules should

10.1021/jp065016b CCC: $37.00
Published on Web 01/18/2007

CHART 1: (Left) Pictorial Representation of a G2 Dendrimer Illustrating the Difference between Outer Pocket and One-Layer-Inner Pocket[a] and (Right) DF41 Fragment Where Y = Functional Group (−OH in This Work)

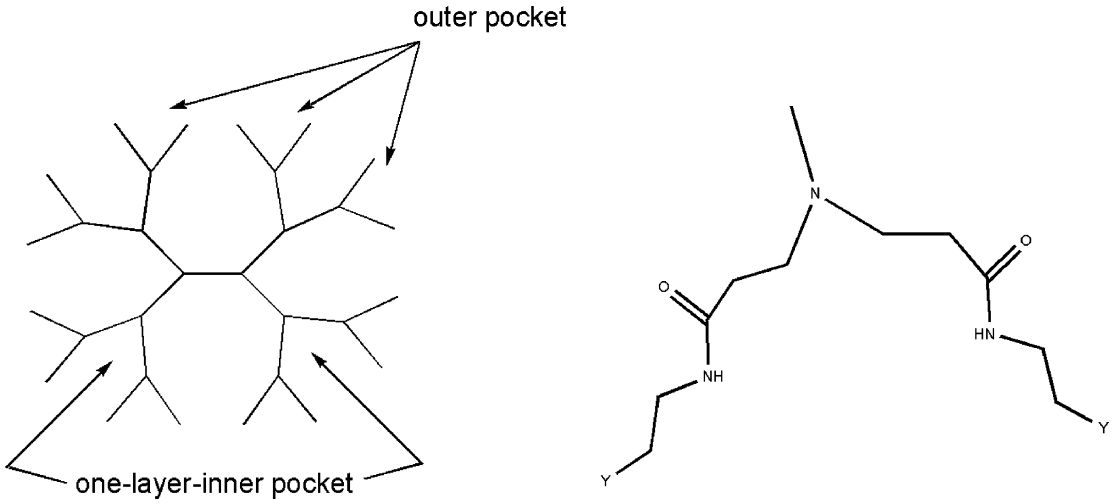

[a] Outer pockets are the outermost pockets limited by two branches. One-layer-inner pockets are also limited by two branches but locate closer to the core (center) of the dendrimer.

overcome interactions with *outer pockets* (Chart 1); these interactions are more likely to be local due to pocket encapsulation of any of the six guest species considered: $PtCl_4^{2-}$, $PtCl_3(H_2O)^-$ and $PtCl_2(H_2O)_2$ in *cis* and *trans* forms, and the counterions K^+ and Cl^-. Therefore we use dendrimer fragment models instead of a model of a complete dendrimer, especially one of generation larger than G0, currently intractable by QM methods.

Dendrimer fragments are suitable to properly describe the region of interest. The first fragment model, DF41, has been introduced in previous work (Chart 1): DF stands for "Dendrimer Fragment" followed by the number of atoms the fragment is made out of. Structurally, DF-41 is similar to a fragment we used previously,[18] consisting of two branches stemming out of a tertiary amine nitrogen but completing the nitrogen three-coordination with a methyl group rather than with a H atom. This model is helpful to describe an unprotonated pocket. In addition, because a low pH affects the structure of the dendrimer,[19] we also study a DF41-H fragment defined as a DF41 fragment with a proton located on top of the tertiary amine N. This simplified approach is intended to be the first step toward gaining new insights and details in the noncovalent binding of molecular species to larger dendrimers.

The B3LYP hybrid flavor of density functional theory (DFT) along with Hay and Wadt pseudopotentials[20] for Pt and the 6-31+g(d) basis set for all other atoms are used along this work for interactions between anions and uncharged particles with dendrimer sites. Although not all our modeled species are anions, for the sake of consistency we have used this method when calculating cations and neutral species. This method was used and reported in a previous paper.[15]

Optimized geometries corresponding to minimum energy configurations were obtained with the Gaussian03 suite of programs;[21] the nature of the stationary points was tested with frequency calculations that also provide the zero point energy and the thermal and free energy corrections to the electronic energy within the harmonic approximation. However, the finding of absolute values of thermodynamic quantities for a given noncovalent binding (NCB) reaction is not claimed in this work, but they provide qualitative insights on the feasibility of those reactions.

Additional insights on the mode of binding might be obtained by MD simulations. However they are expected to be computationally very expensive due to the extensive sampling required,[15] unless some constraints are applied. Second, as the breaking of bonds is not allowed in classical MD with nonreactive force fields, the use of reactive force fields may turn out imperative consequently increasing the computational cost.

3. Results

In previous work[15] we determined using a thermodynamic analysis that an *unprotonated* pocket (host) was able to host two, and perhaps three, water molecules (guest). Although thermodynamics cannot offer insights on whether a dynamic exchange of these water molecules with other water molecules outside the host may occur, we expect to better understand the feasibility of a guest exchange when such a guest is other than water. For the metal complex, noncovalent binding[22] (NCB) involves no exchange of first shell ligands (either Cl^- or H_2O) during the initial course of their interaction with the dendrimer pocket. However, exchange of chloride or water will take place after NCB, in what is known as the ligand exchange reaction (LER), once the corresponding energetic barriers are overcome. An investigation of LER is reported elsewhere. In this work, energies of reaction (ΔE_0, ΔH and ΔG) of displacement reactions that model this exchange have been calculated. Also, by comparing these reaction energies with those of processes where the host is absent we have defined the terms "binding affinity" and "relative binding affinity". Thus, the term "binding affinity" refers to the likelihood of a particular displacement reaction (in kcal/mol) whereas "relative binding affinity" refers to a ratio of two displacement reactions (dimensionless number).

A continuum approach was not used to represent the environment surrounding the pocket because outer pockets in dendrimers are not surrounded by a medium with uniform dielectric constant.[15] Rather, in selected cases the solvent effect was addressed by calculation of the reaction energies considering a hydrated guest rather than a naked one.

3.1. Binding Affinity for Water. In this section, we report the binding affinity of several molecular species B with charge *m* toward a free water dimer by calculating their energetics in the following reactions.

TABLE 1: Electronic Energies with ZPE Correction (E_0), Enthalpies and Free Energies of Reaction According to Eq 1[a]

species	ΔE_0	ΔH	ΔG
K^+	−14.4	−13.6	−14.4
$\{K\text{-}(H_2O)\}^+$	−11.4	−10.7	−11.4
$\{K\text{-}(H_2O)_2\}^+$	−9.5	−8.8	−9.7
Cl^-	−9.7	−9.9	−10.8
OH^-	−24.6	−25.1	−24.3
$PtCl_4^{2-}$	−12.2	−12.0	−10.0
$PtCl_3(H_2O)^-$	−7.9	−8.3	−4.2
cis-$PtCl_2(H_2O)_2$	−6.8	−7.1	−4.3
trans-$PtCl_2(H_2O)_2$	−9.7	−9.9	−6.6
DF41	−4.9	−4.7	−2.0
DF41-H^+_a	−2.9	−3.1	0.4
DF41-H^+_b	−8.0	−8.2	−4.3

[a] Values in kcal/mol. Subscripts a and b indicate two different configurations of the protonated fragment DF41-H^+ (see text).

TABLE 2: Electronic Energies with ZPE Correction (E_0), Enthalpies and Free Energies of Reaction According to Eq 2[a]

species	ΔE_0	ΔH	ΔG
K^+	−15.4	−15.3	−9.4
$\{K\text{-}(H_2O)\}^+$	−13.4	−13.3	−7.7
$\{K\text{-}(H_2O)_2\}^+$	−11.3	−11.2	−4.8
Cl^-	−12.4	−13.2	−4.4
OH^-	−20.9	−21.5	−14.0
$PtCl_4^{2-}$	−15.0	−15.5	−6.8
$PtCl_3(H_2O)^-$	−9.7	−10.4	−0.94
cis-$PtCl_2(H_2O)_2$	−11.2	−11.9	−2.9
trans-$PtCl_2(H_2O)_2$	−12.8	−13.7	−3.6
DF41	−9.0	−9.7	−0.82
DF41-H^+_a	−9.9	−10.1	−1.6
DF41-H^+_b	−11.9	−12.9	−2.2

[a] Values in kcal/mol. Subscripts a and b indicate two different configurations of the protonated fragment DF41-H^+ (see text).

Formation of monohydrated species B:

$$B^m + (H_2O)_2 \rightarrow [B(H_2O)]^m + H_2O \quad (1)$$

Hydration of monohydrated species B:

$$[B(H_2O)]^m + H_2O \rightarrow [B(H_2O)_2]^m \quad (2)$$

The protonated reactants listed in the last two rows of Tables 1 and 2 deserve further explanation. For each ΔE_0, ΔH or ΔG, the values in Table 1 are calculated with respect to the lowest energy configuration of a tertiary amine N-protonated fragment DF41-H^+ (fragment RefCoB in Figure 6, ref 15). Two distinct configurations are obtained: DF41-H_3O^+, where a water molecule binds to the proton (DF41-H^+_a), and DF41-H^+-H_2O, where water binds to the hydroxyl terminal groups (DF41-H^+_b). The last one is the most stable configuration (ΔG: −4.3 kcal/mol) according to eq 1. Taking these two structures as reference, water molecules are added according to eq 2, yielding DF41-H_3O^+-H_2O, a configuration where the additional water binds inside the pocket and DF41-H^+-$(H_2O)_2$ (configuration 2C*; see Figure 2; for further details see also ref 15), where a water dimer forms and binds to the hydroxyl terminal groups in a water-tetramer like form (Figure 2).

3.2. Binding Affinity for Hydronium. A water molecule rather than a hydronium ion is most likely to be released when a given species encounters a monohydrated hydronium. Equation 4 describes the formation of a *protonated* monohydrated species B with charge *m* with water as subproduct. The thermodynamic values are reported in Table 3.

Formation of *protonated* monohydrated species B:

$$B^m + (H_2O)(H_3O)^+ \rightarrow B^m(H_3O)^+ + H_2O \quad (4)$$

3.3. Binding Affinity for Water Hosted by a Tertiary Amine N-Protonated Pocket. In sections 3.1 and 3.2 we presented energetics of reaction of species B with a free water dimer and "protonated water dimer". In this section we discuss the energetics for a reaction where species B is exchanged with a water molecule from the water dimer hosted by a dendrimer pocket. Thus, we expect to gain insight on the effect of the host over the binding of its guests to water.

From the group of guest species analyzed in the previous sections, only K^+ was excluded from this study due to its positive charge. By calculating the "relative binding affinity" of a given species for water dimer in the presence of the host pocket and comparing it to those calculated in sections 3.1 and 3.2 (in the absence of the pocket), we can determine whether or not a particular species will be able to reach the pocket and stay bound there. As this section copes with interactions of DF41-H with other species, we chose the configuration 2C* (see Figure 2, section 3.1) as the reference (reactant side) for the calculation of reaction energies according to eq 5.

Formation of monohydrated species B inside tertiary amine N-protonated pocket:

$$[\{DF41\text{-}H\}(H_2O)_2]^+ + B^m \rightarrow [\{DF41\text{-}H\}B(H_2O)]^{m+1} + H_2O \quad (5)$$

Equation 5 is a process analog to eq 4 reported in section 3.2. However, only results for eq 5 are reported in Table 4. The lowest energy configuration structures for the product $[\{DF41\text{-}H\}B(H_2O)]^{m+1}$ are shown in Figure 3.

3.4. Binding Affinity for Water in an Unprotonated Pocket. In this section, reaction energies are calculated assuming that the structure [DF41-$(H_2O)_2$] (configuration 2C in ref 15 represents an encapsulated water dimer reacting with species B (with charge *m*) in the following displacement reactions. The results for eq 6 are given in Table 5. Binding affinity calculations were done not only for K^+ but also for the anions and uncharged species.

Formation of monohydrated species B inside *unprotonated* pocket:

$$[DF41\text{-}(H_2O)_2] + B^m \rightarrow [DF41\text{-}B(H_2O)]^m + H_2O \quad (6)$$

3.5. Hydration of Counterions in Unprotonated Pockets. We have shown that water can be hosted by both *unprotonated* and *protonated* pockets,[15] and the present results suggest that other species can be also hosted along with at least one water (section 3.4).

Succesive hydration of DF41-B^m:

$$DF41\text{-}B^m(H_2O)_n + (H_2O)_2 \rightarrow [DF41\text{-}B^m\text{-}(H_2O)_{n+1}] + H_2O \quad (7)$$

Unlike eq 5 where a pocket hosting water exchanges one of them for an incoming guest, eq 7 begins with the assumption that DF41-B^m is formed ($n = 0$) and then additional water molecules $(H_2O)_n$ bind in a hydration-like manner. Thus, we study hydration of Cl^- and K^+, which are simpler to be tested compared with Pt(II) metal complexes due to their smaller size and complexity. Because (as will be seen in section 4.2) the relative binding affinity (for water inside the pocket) of OH^-

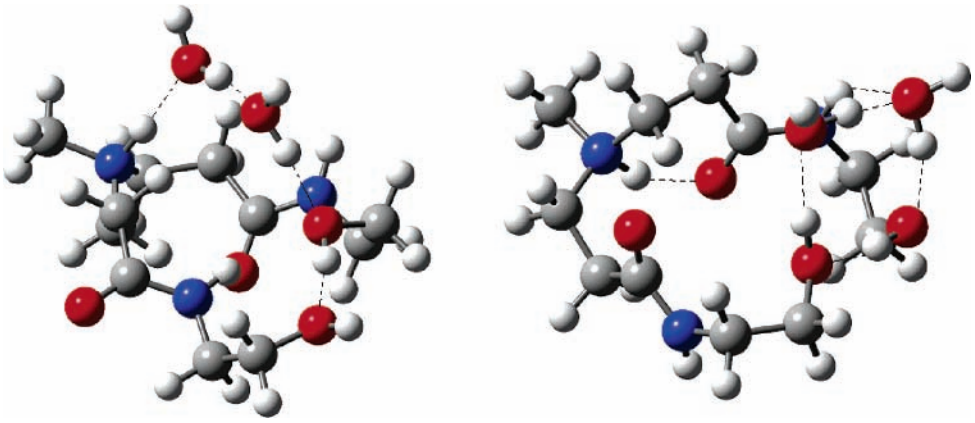

Figure 2. Configurations of tertiary amine N-protonated outer pocket hosting a water dimer. Left: DF41-H_3O^+-H_2O. Right: DF41-H^+-$(H_2O)_2$ (configuration 2C*) (see text). Reprinted from ref 15 (part 1 of this series).

TABLE 3: Electronic Energies with ZPE Correction (E_0), Enthalpies and Free Energies of Reaction According to Eq 4[a]

species B	ΔE_0	ΔH	ΔG
Cl^-	−132.8	−131.9	−135.3
OH^-	−192.6	−191.7	−194.3
$PtCl_4^{2-}$	−181.7	−181.5	−179.3
$PtCl_3(H_2O)^-$	−86.8	−85.9	−84.8
cis-$PtCl_2(H_2O)_2$	−1.6	−0.9	−0.4
trans-$PtCl_2(H_2O)_2$	−5.1	−4.3	−3.4
DF41	−60.4	−59.9	−57.4

[a] Values in kcal/mol.

TABLE 4: Electronic Energies with ZPE Correction (E_0), Enthalpies and Free Energies of Reaction for the Formation of Monohydrated Species B Inside Protonated Pocket, According to Eq 5[a]

species B	ΔE_0	ΔH	ΔG
Cl^-	−86.7	−85.5	−89.6
OH^- [b]	−132.1	−131.2	−134.6
$PtCl_4^{2-}$	−146.2	−144.5	−143.5
$PtCl_3(H_2O)^-$	−54.4	−52.9	−52.1
cis-$PtCl_2(H_2O)_2$	−1.3	−0.3	2.6
trans-$PtCl_2(H_2O)_2$	2.2	2.7	7.2

[a] Values in kcal /mol. [b] This structure is indeed {DF41-H_2O-(H_2O)} (OH^- binds to H^+ to yield H_2O) instead of {DF41-H}OH-(H_2O).

is lower than those of K^+ and Cl^-, OH^- is excluded from the discussion here. Also, as the concentration of OH^- is low at neutral or lower pH, its probability to interact with water should decrease accordingly. This is not the case with the other counterions. For instance, the K^+ concentration is 2-fold the initial concentration of the precursor salt.

Table 6 presents the reaction energies according to eq 7 corresponding to the lowest energy configurations (in a few cases only one was found) at a given degree of hydration.

ΔE_0 and ΔG for the reaction DF41 + $K^+ \rightarrow$ DF41-K^+ are −45.0 and −40.5 kcal/mol, respectively, whereas for the reaction DF41 + $Cl^- \rightarrow$ DF41-Cl^- they are −40.5 and −36.2 kcal/mol. Although the additional binding of water is not as exothermic as these reactions, it is still significant particularly for the first water of hydration: if DF41-{$K(H_2O)$}$^+$ is formed, ΔE_0 and ΔG are −18.8 and −11.3 kcal/mol, respectively (Table 6). However, when DF41-{$Cl(H_2O)$}$^-$ is formed by a similar reaction, the values for ΔE_0 and ΔG are much lower: −4.9 and −0.21 kcal/mol, respectively.

In DF41-{$K(H_2O)$}$^+$, K^+ binds to two amide O, one hydroxyl O and a water O, all of them in relatively equatorial positions, with bond lengths ranging 2.61−2.97 Å, the shorter distance being for K^+−O water, whereas the K^+−tertiary amine (N3) distance is longer (3.90 Å). On the other hand, in DF41-{Cl-(H_2O)}$^-$ (Figure 5), Cl^- binds to two hydroxyl H, one water H, two amide H and perhaps to two methylene H's. Bond distances range from 2.30 (hydroxyl H) to 3.01 Å (methylene H). Therefore coordination number of 5−7 for the chloride ion can be inferred. This is in agreement with experimental results.[23] For both of these structures, the additional water molecule completes the first shell coordination of the ion.

Beyond the first water molecule, K^+ and Cl^- accept waters but not in their first coordination shell. Thus, the additional water in DF41-{$Cl(H_2O)$}$^-$ joins two hydroxyl oxygen atoms and faces toward the outside of the pocket. Additional water in K^+ can still be added axially, with bond distances ranging 2.62−3.08 Å, the longer being the distance first-added O water−K^+. Binding of a third water is still favorable and the bond distances range from 2.62 to 2.77 Å (the longer for amide O−K^+). The first- and second-added water stay outside the first coordination shell (Figure 5). The K^+−N3 bond distance elongates to 4.02 Å. Therefore no binding to N3 is inferred. Table B with all distances and angles is provided as Supporting Information.

Further addition of water is thermodynamically unfavorable: bond distances range 2.69−2.98 Å (the longer distance corresponds to the interaction with two waters) and one water molecule locates in the second coordination shell. Our results point out that K^+ is at least tetracoordinated when it interacts with the pocket, in agreement with experiments done in proteins.[24] It is also observed that when K^+ enters the pocket with water, the O−O distance ranges 4.44−4.65 Å; and the OT−OT distance ranges 4.66−11.72 Å. A series of angles help to characterize the outer pocket in relation to the orientation of their amide O atoms: angle γ, formed by amide O1(branch 1)−tertiary amine N3−amide O2(branch 2); angle α, formed by carbonyl CO1(branch 1)−N3−carbonyl CO2(branch 2). The α angle ranges 115.7−125.9°; the γ angle ranges 81.8−87.6°.

4. Discussion

Results from sections 3.1 and 3.4 are compared in section 4.1 to investigate the effect of protonation on the binding of guests inside an outer pocket. Results from sections 3.2 and 3.3 are discussed in section 4.2 with the goal of analyzing the effect of hydration on the binding of species (other than water) to a water dimer as well as how this binding affinity is affected in the presence of an outer pocket. Finally, in section 4.3 we attempt to rationalize the results of section 3.5 so that we can gain insight into conformational changes in the outer pocket configuration needed for the hosting of particular guests.

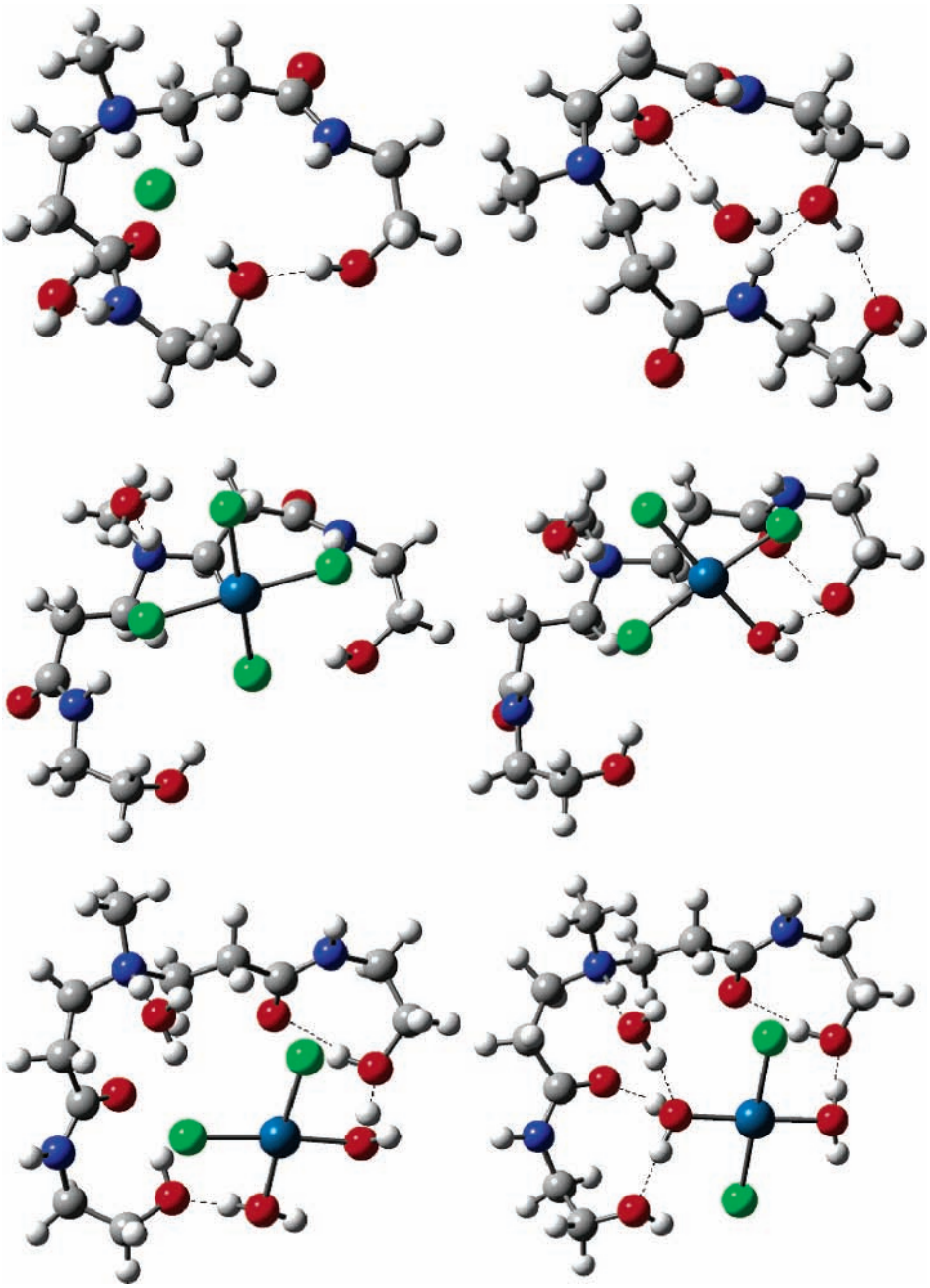

Figure 3. Lowest energy configurations for $\{(DF41\text{-}H)B(H_2O)\}^{m+1}$ with m the charge of species B (guest) interacting with a PAMAM outer pocket (host). Upper left: $\{DF41\text{-}H/Cl\text{-}(H_2O)\}^-$ with HO−OH 1.88 Å, NH−OH_2 1.96 Å. Upper right: DF41-H_2O-(H_2O). The initial configuration for this structure had proton and hydroxyl ion separated by a water molecule. The optimized structure shows that the proton migrated to the neighboring water; on the other hand, this water molecule donates a proton to the hydroxyl anion producing another water molecule. Hydrogen bonds: N−HOH 1.84 Å, H_2O−HN 2.21 Å, H_2O−HOH 1.92 Å, H_2O−OH 1.95 Å, NH−OH 2.03 Å and OH−OH 1.83 Å. Middle left: $\{DF41\text{-}H/PtCl_4\text{-}(H_2O)\}^-$ with NH^+−HOH 1.76 Å. Middle right: $\{DF41\text{-}H/PtCl_3\text{-}(H_2O)\}$ with NH^+−HOH 1.72 Å, Pt(II)−OH_2−OH 1.72 Å, OH−O 2.09 Å. Lower left: $\{DF41\text{-}H/cis\text{-}PtCl_2(H_2O)(H_2O)\}^+$ with NH^+−HOH 1.73 Å, OH−O 1.82 Å and two Pt(II)−OH_2−OH 1.61 and 1.59 Å. Lower right: $\{DF41\text{-}H/trans\text{-}PtCl_2(H_2O)(H_2O)\}^+$ with NH^+−HOH 1.78 Å, OH−O 1.86 Å, two Pt(II)−OH_2−OH 1.65 and 1.61 Å, Pt(II)−H_2O−H_2O 1.84 Å and Pt(II)−OH_2−O 1.70 Å.

4.1. Effect of Tertiary Amine N-Protonated Pocket (Host) on the Binding of Guest Species. Reaction energies for formation of *protonated* monohydrated species or binding affinity for monohydrated hydronium for all species studied but potassium ion, are shown in Table 3 (vide supra). It is evident that electrostatic attraction between an anion such as $PtCl_4^{2-}$ and H_3O^+ will be strong; yet it was found to be lower than that of OH^- despite the $PtCl_4^{2-}$ charge being double that of OH^-. On the other hand, H_3O^+ interaction with uncharged species like $PtCl_2(H_2O)_2$ is weaker and a tradeoff between the attraction exerted by negatively charged ligands such as Cl^- and the repulsion between Pt^{2+} and the H_3O^+ hydrogen atoms is evident. As a result, a difference between *cis*- and *trans*-$PtCl_2(H_2O)_2$ binding affinity can be observed due to their different geometries. Considering only the uncharged complexes in absence of host, the binding affinity for monohydrated hydronium follows the order *unprotonated* pocket ≫ *trans*-$PtCl_2(H_2O)_2$ > *cis*-$PtCl_2(H_2O)_2$, whereas among the species charged with −1 it follows the order: $OH^- > Cl^- > PtCl_3(H_2O)^-$.

Regarding interactions with a *protonated* pocket (host), the binding affinity strength (Table 4) reverts for uncharged species: *cis*-$PtCl_2(H_2O)_2$ > *trans*-$PtCl_2(H_2O)_2$ with respect to

TABLE 5: Electronic Energies with ZPE Correction (E_0), Enthalpies, and Free Energies for Hydration of Monohydrated Species B Inside *Unprotonated* Pocket, According to Eq 6[a]

species B	ΔE_0	ΔH	ΔG
K^+	−49.3	−47.9	−49.0
$\{K\text{-}(H_2O)\}^+$	−41.0	−40.0	−39.5
$\{K\text{-}(H_2O)_2\}^+$	−35.4	−35.1	−30.5
Cl^-	−31.5	−30.7	−33.6
OH^-	−62.3	−63.0	−60.4
$PtCl_4^{2-}$	−36.8	−35.9	−32.9
$PtCl_3(H_2O)^-$	−12.0	−11.2	−8.0
cis-$PtCl_2(H_2O)_2$	−10.3	−10.2	−5.0
trans-$PtCl_2(H_2O)_2$	−11.9	−12.1	−5.4

[a] Values in kcal/mol.

TABLE 6: Electronic Energies with ZPE Correction (E_0), Enthalpies, and Free Energies for the Successive Hydration of DF41-B[m], According to Eq 7[a]

product	config	ΔE_0	ΔH	ΔG
DF41-$\{K(H_2O)\}^+$	1A	−18.2	−18.8	−11.3
DF41-$\{K(H_2O)_2\}^+$	2A	−6.1	−5.7	−5.0
DF41-$\{K(H_2O)_3\}^+$	3A	−5.7	−5.9	−2.4
DF41-$\{K(H_2O)_4\}^+$	4A	−3.2	−3.4	1.7
DF41-$\{Cl(H_2O)\}^-$	1A	−4.9	−5.2	−0.21
DF41-$\{Cl(H_2O)_2\}^-$	2A	−4.4	−4.5	−1.5

[a] Values in kcal/mol.

the affinities for the free monohydrated hydronium, whereas although the binding affinity of $PtCl_4^{2-}$ is larger than that of OH^- the same order of binding is found for species charged with −1: $OH^- > Cl^- > PtCl_3(H_2O)^-$.

Next we assume that the relative probability of finding a particular species in either of two scenarios: inside or outside of the pocket, is proportional to their energy ratio: ΔE(*protonated* pocket)/ΔE(outside of pocket) where the energies correspond to the reaction energies in Tables 4 and 3, respectively. The energy ratios are summarized in Table 7. *cis*- and *trans*-$PtCl_2(H_2O)_2$ have a very small binding affinity for monohydrated hydronium (Table 3, vide supra) and a low or even positive ΔG (Table 4, vide supra). Therefore their energy ratio was not included in Table 7. This suggests that tertiary amine N-protonated pockets are not able to attract neutral species, such as *cis*- and *trans*-$PtCl_2(H_2O)_2$.

The energy ratios shown in Table 7 suggest that $PtCl_4^{2-}$ (ratio 0.8) is slightly more likely to interact with a protonated pocket than Cl^-, OH^- and $PtCl_3(H_2O)^-$ (ratios 0.6−0.7). Nonetheless, because all these ratios are lower than 1.0, it is expected that these species prefer to interact mainly with H_3O^+ in the surrounding medium outside of the pocket. This finding suggests why protonation does not help complexation at moderate[11] precursor concentrations. For comparison, it is interesting to note that the values of the reaction free energies of Cl^- and OH^- in protonated pockets are of the same order of magnitude of their hydration energies in their fully solvated states.[25] This suggests that the protonated pocket exerts a comparable interaction to that of a polar solvent; however, such interaction is weaker than that with a free monohydrated hydronium ion as may exist in the solution medium surrounding the dendrimer.

4.2. Effect of *Unprotonated* Pocket (Host) on the Binding of Guest Species. Reaction Gibbs free energies corresponding to the formation of monohydrated species or binding affinity

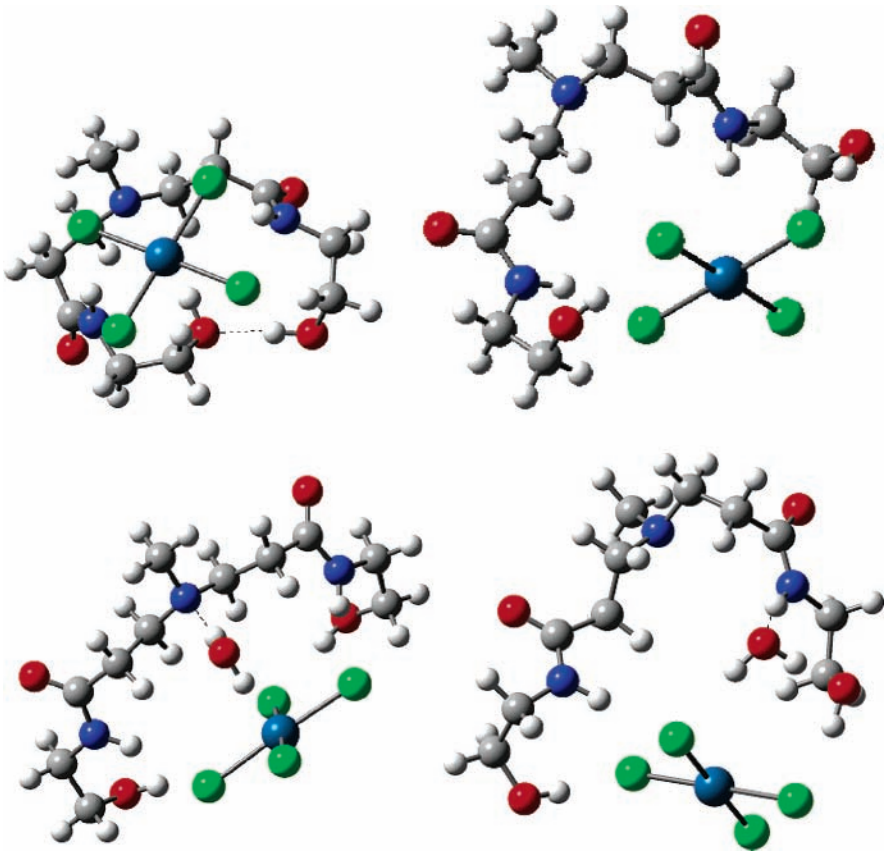

Figure 4. Upper left: DF41-$PtCl_4^{2-}$. "Outside but attached to the pocket" configuration. Pocket remains closed with terminal hydroxyl groups binding with a hydrogen bond OH−OH of 1.83 Å Upper right: "Inside pocket" lec configuration. Opening of the pocket is evident. Lower left: DF41-H_2O−$PtCl_4^{2-}$, with tertiary N−HOH 2.05 Å. Lower right: DF41-H_2O−$PtCl_4^{2-}$, with amide N−HOH 1.91 Å. The energy difference between the two structures in the bottom row is 0.2 kcal/mol (ΔG). Orientation of their amide O atoms in both branches is found to point outwardly in relation to the pocket.[15]

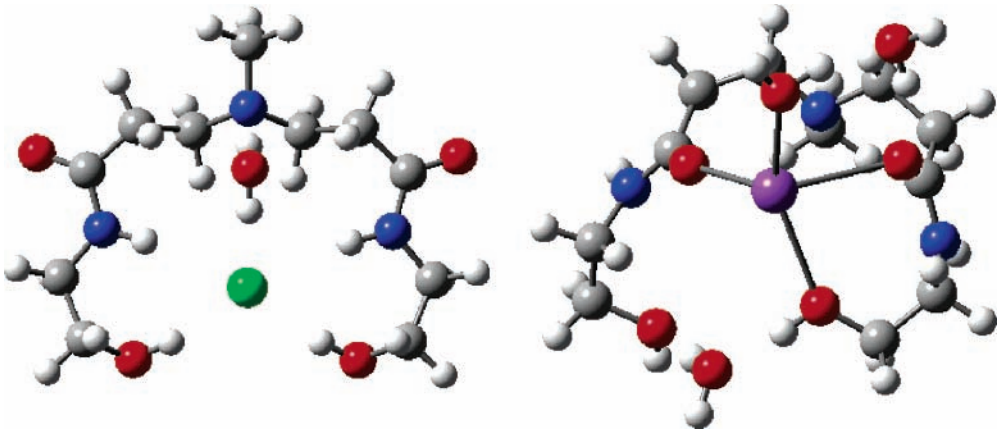

Figure 5. Left: $[DF41\text{-}Cl^{-}(H_2O)]^{-}$. Right: $[DF41\text{-}K\text{-}(H_2O)_3]^{+}$

TABLE 7: Ratio ΔE(Protonated Pocket)/ΔE(Outside of Pocket), Based on Data from Tables 4 and 3[a]

	energy ratios		
species	ΔE_0	ΔH	ΔG
Cl^{-}	0.7	0.6	0.7
OH^{-}	0.7	0.7	0.7
$PtCl_4^{2-}$	0.8	0.8	0.8
$PtCl_3(H_2O)^{-}$	0.6	0.6	0.6

[a] Each column corresponds to an energy ratio involving ΔE_0, ΔH, and ΔG, respectively.

for water dimer (Table 1, vide supra) are larger than those of the hydration of these monohydrated species (Table 2), except for DF41 and DF41-H^{+}_a. Tables 1 and 2 also show that the high binding affinity of K^{+} for water decreases when the number of added solvation molecules increases. This trend is similar in almost all the other species (Figure 6 and Table B in Supporting Information) but is more dramatic for OH^{-}.

On the other hand, Table 5 illustrates how the host affects the binding affinity of hydrated potassium species for a *pocketed water dimer*, which binds strongly within pockets; yet the more solvation molecules surrounding the ion, the less feasible the retention of water already present in the pocket (exchange) or the binding of additional water without pocket involvement (hydration).

Considering only the free uncharged complexes according to eq 1, the binding affinity for water dimer (Table 1) follows the order *trans*-$PtCl_2(H_2O)_2$ > *cis*-$PtCl_2(H_2O)_2$ > unprotonated pocket, whereas among the species charged with −1, the water binding affinities of OH^{-} and Cl^{-} are higher than that of $PtCl_3(H_2O)^{-}$. In spite of its higher charge, the $PtCl_4^{2-}$ binding affinity for water is comparable with that of Cl^{-}.

When interactions with an *unprotonated* pocket (host) are considered, the binding affinity (Table 5) in uncharged complexes for a pocketed water dimer follows the order *trans*-$PtCl_2(H_2O)_2$ > *cis*-$PtCl_2(H_2O)_2$ whereas among species charged with −1 the order is OH^{-} > Cl^{-} > $PtCl_3(H_2O)^{-}$. The binding affinity of $PtCl_4^{2-}$ for pocketed water is lower than that of OH^{-} although similar to that of Cl^{-}. Thus, whether the host is present or not the affinity strength follows a similar ordering.

As in section 4.1, the relative probability of finding a particular species inside or outside of the pocket, is assumed to be proportional to their energy ratio (ΔE(*unprotonated* pocket)/ΔE(outside of pocket)). This energy ratio or relative binding affinity for water dimer, defined as the ratio between the reaction energies calculated with eq 6 (formation of monohydrated species B inside unprotonated pocket) and eq 1 (formation of mono-

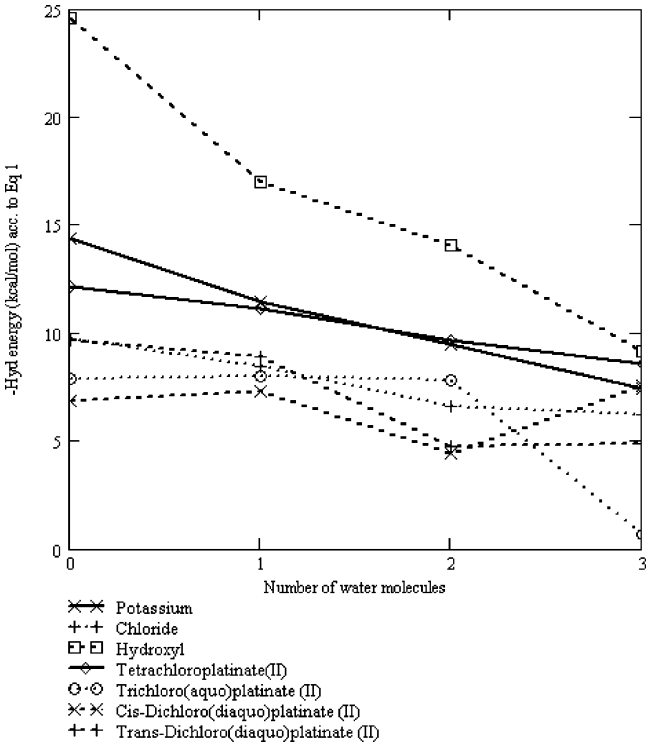

Figure 6. Hydration energy (ΔE_0 according to this equation: $B(H_2O)_n + (H_2O)_2 \rightarrow B(H_2O)_{n+1} + H_2O$) vs number of water molecules in the reactant. The negative of the value of the energy is plotted in the *y*-axis so that a decreasing ability toward hydration is observed in almost all ions and particularly in OH^{-}. Note: Data for Pt(II) complexes has been extracted from ref 15 and the rest correspond to this work.

hydrated species B outside unprotonated pocket), is shown in Table 8. It could also be regarded as a partition coefficient among two scenarios (pocket vs outside of pocket) and can consequently provide qualitative insight into the ability of the pocket to host particular guests.

The energy ratios shown in Table 8 suggest that host−guest interactions in the unprotonated pocket are much stronger than those between water and the guest (in the absence of the host). All ratios are higher than 1.0 except the ΔG ratio for *trans*-$PtCl_2(H_2O)_2$. Also, Table 8 clearly suggests that $PtCl_4^{2-}$ is a suitable competitor of K^{+} and Cl^{-} for the pocket sites.

Next we define new relative binding affinities as the ratios of energies (ΔE_0, ΔH, ΔG) for hydration of species B inside an *unprotonated* pocket (according to eq 6) over the sum of the energies given by eq 1 (formation of monohydrated species B without *unprotonated* pocket) and eq 2 (hydration of mono-

TABLE 8: Ratio ΔE(Unprotonated Pocket)/ΔE(Outside of Pocket), Based on Data from Tables 1 and 5[a]

species B	energy ratios		
	ΔE_0	ΔH	ΔG
K^+	3.4	3.5	3.4
$K\text{-}(H_2O)^+$	3.6	3.7	3.5
$K\text{-}(H_2O)_2^+$	3.7	4.0	3.1
Cl^-	3.2	3.1	3.1
OH^-	2.5	2.5	2.5
$PtCl_4^{2-}$	3.0	2.9	3.3
$PtCl_3(H_2O)^-$	1.5	1.4	1.9
cis-$PtCl_2(H_2O)_2$	1.5	1.4	1.1
trans-$PtCl_2(H_2O)_2$	1.2	1.2	0.8

[a] Each column corresponds to an energy ratio involving ΔE_0, ΔH, and ΔG, respectively.

TABLE 9: Ratio ΔE(Unprotonated Pocket)/ΔE(Outside of Pocket), Based on Data from Tables 1, 2 and 5[a]

species B	energy ratios		
	ΔE_0	ΔH	ΔG
K^+	1.7	1.7	2.1
$K\text{-}(H_2O)^+$	1.7	1.7	2.1
$K\text{-}(H_2O)_2^+$	1.7	1.8	2.1
Cl^-	1.4	1.3	2.2
OH^-	1.4	1.4	1.6
$PtCl_4^{2-}$	1.4	1.3	2.0
$PtCl_3(H_2O)^-$	1.4	0.6	1.5
cis-$PtCl_2(H_2O)_2$	0.6	0.5	0.7
trans-$PtCl_2(H_2O)_2$	0.5	0.5	0.5

[a] Each column corresponds to an energy ratio involving ΔE_0, ΔH, and ΔG, respectively.

hydrated species B without *unprotonated* pocket). The rationale for this division is that the negative free energies calculated with eq 2 indicate that such reaction of species B with a water dimer (eq 1) will continue according to eq 2.

The calculated ratios shown in Table 9 are lower than those in Table 8. These new ratios indicate also that not only *trans*-$PtCl_2(H_2O)_2$ but also its *cis* isomer are less likely to be encapsulated within an *unprotonated* pocket (both ratios for these species are lower than 1.0). The relative binding affinity (energy ratio) of OH^- is lower than those of K^+, Cl^- and $PtCl_4^{2-}$, although similar to that of $PtCl_3(H_2O)^-$. Aside from this, Table 9 expresses the trend described by Table 8.

This analysis suggests that any charged species will prefer binding inside rather than outside an *unprotonated* outer pocket. To illustrate and test this conclusion, several configurations of DF41-$PtCl_4^{2-}$ were optimized and two of them were selected: the lowest energy configuration (lec) for a tetrachloroplatinate-(II) hosted inside a pocket (Figure 4, upper right) and another with the ion located outside but attached to the pocket (Figure 4, upper left). A reaction energy defined as $\Delta E_0 = E_0$(DF41-$PtCl_4^{2-}$) $- \{E_0$(DF41) $+ E_0(PtCl_4^{2-})\}$ yielded -45.0 and -35.0 kcal/mol for the "inside pocket" and the "outside but attached to the pocket" configurations, respectively. The ratio of these energies is larger than 1.0, suggesting conclusions similar to those from Tables 8 and 9: it is more likely for charged species to bind inside rather than outside *unprotonated* pockets. Therefore, it is reasonable to assume that after initial interaction of $PtCl_4^{2-}$ with the outer pockets exposed to bulk water, the precursor anion will bind inside the pocket.

Figure 4 shows that although the outer pocket remained closed, as evidenced by the OH−OH hydrogen bond, interactions between Cl^- ligands and amide H still occur. As the relevant energetic barriers, involving most likely local configuration changes, are overcome, it may bind inside the pockets. In this configuration, additional interactions with hydroxyl hydrogen appear, suggesting that they are stronger than the OH−OH hydrogen bonds.

4.3. Conformational Change in Outer Pockets upon Interaction with Guests. In a previous paper[15] we postulated three ideal configurations for outer pockets based on the relative orientation of their amide oxygen atoms with respect to the pocket. If both pointed inside, or one inside and the other outside, or both outside, the configurations were named inward−inward, inward−outward and outward−outward, respectively. The preferred configuration will resemble one of these more closely than others and to that effect a geometrical analysis was made.

The range of variation of several geometric parameters for configurations of K^+ and water binding in an *unprotonated* pocket (section 3.5) was compared with the values for binding of water alone,[15] observing first that the amide O−O bond distances in the first case are shorter, and that their range of variation is narrower. Also, at their minimum, the terminal groups OT−OT bond distance is longer, suggesting the absence of hydrogen bond between hydroxyl terminal groups, and the values of the angle α (defined in section 3.5) as well as those of the angle γ (defined in section 3.5) are significantly lower and have a narrower range of variation. All these observations point to the fact that cations like K^+ induce the orientation of both amide O atoms in the pocket into inward−inward positions.

A similar comparison made for the binding of Cl^- to the pocket with respect to the values for water-unprotonated pocket structures[15] indicates that the O−O bond distance is larger, the minimum OT−OT is larger and therefore no H-bond between hydroxyl terminal groups exists, values of the angle α are within the range measured for water-unprotonated pocket structures, and the value of γ angles is significantly larger. The longer O−O bond distances and values for the angle γ point to the fact that anions like Cl^- induce orientation of both amide O atoms into outward−outward positions.

These results hint to a markedly different configurational rearrangement of the outer pockets, and consequently of the larger dendrimer, when either positively or negative charged ions are hosted. This is less obvious for asymmetric guest structures, whether on charge distribution or geometry, than for symmetric ones.

Therefore reorientation of branches in the dendrimer (pocket regions) has to occur before a given species is hosted inside a pocket. For instance, although Cl^- is a suitable competitor for $PtCl_4^{2-}$ species and both bear negative charges, none of them yields an inward−outward. As the preferred configuration when only water is hosted inside *unprotonated* packets is inward-outward,[15] then configurational rearrangement in the dendrimer will take place to allow other guest species in.

5. Conclusions

Tertiary amine-N protonated pockets are not likely to host neutral species like *cis*- and *trans*-$PtCl_2(H_2O)_2$, but only anions. Yet the fact that no species among the anions studied has a larger binding affinity for encapsulated water than for a monohydrated hydronium might explain why complexation of Pt(II) with the PAMAM dendrimer has not been observed, to the best of our knowledge, in protonated dendrimers.[11]

The binding affinity of the species studied for the water dimer decreases upon hydration. The effect of solvent inside pockets has not been possible to study for Pt(II) complexes but only for K^+ showing the same trend. However, binding affinity increases when reacting with a water dimer encapsulated within

an *unprotonated* pocket and although all species can bind to it, not all do it with the same strength. For instance, host−guest interactions are weak when the guest is either *cis*- or *trans*-$PtCl_2(H_2O)_2$ but strong when such guests are either K^+, Cl^- or $PtCl_4^{2-}$ that have a similar relative binding affinity. The relative binding affinity order is $K^+ \sim PtCl_4^{2-} \sim Cl^- > OH^- > PtCl_3H_2O^- >$ *cis*-$PtCl_2(H_2O) >$ *trans*-$PtCl_2(H_2O)$. Therefore, charged species are more likely to bind inside rather than outside *unprotonated* pockets.

One of the first steps conducive to nanoparticle synthesis is to encapsulate the metal precursor within a template. As it is common to use freshly prepared solutions of K_2PtCl_4, the dominant species will be $PtCl_4^{2-}$. If aquation (conversion of part of $PtCl_4^{2-}$ into its mono- and diaquated species) does not occur during the complexation step, then the main competing counterion will be K^+. On the other hand, knowing that $PtCl_2(H_2O)_2$ binds weakly to outer pockets, and perhaps to dendrimers too, it would not be adequate to use aged and diluted solutions of K_2PtCl_4 that contain predominantly the species in either cis or trans form to obtain nanoparticles. The same rationale ought to apply to other Pt(II) metal precursors that similar species.

Finally, the most notable local configurational change that takes place upon hosting of guest species by a pocket is the orientation of its amide O and depends on the nature of the guest. Upon encapsulation of water[15] one amide O orients inward and one amide O outward, whereas when symmetric, regarding their charge distribution, anions like Cl^- and $PtCl_4^{2-}$ are hosted, both amide O's orient outward. On the other hand, symmetric cation guests trigger inward orientation of both amide O's, as can be inferred from our previous study with Cu^{2+} [18] and along this work with K^+. However, asymmetric species like $PtCl_3(H_2O)^-$ and $PtCl_2(H_2O)_2$ do not follow this trend (see Figure 3). These local configuration changes are likely to affect the configuration of the larger dendrimer the pockets belong to.

In summary, important insights on the complexation ability of dendrimer outer pockets in both a *protonated* and *unprotonated* scenario toward molecular guests have been obtained through thermodynamic and geometric analysis. And, as a result of that, we believe a better understanding of the noncovalent binding (NCB) has been gained. A complementary study on the next step of the complexation, the ligand exchange reaction (LER) will be discussed elsewhere.

Acknowledgment. This work was partially supported by the National Science Foundation grant CTS-0103135 and by the Department of Energy grant DE-FG02-05ER15729. Supercomputer time granted by the National Energy Research Scientific Computing Center (NERSC) and by the DoD Major Shared Resource Centers (ARL MSRC and ASC MSRC) is gratefully acknowledged.

Supporting Information Available: Calculation of the equilibrium distribution of $PtCl_4^{2-}$ and its mono- and diaquated species. Table of distances and bond angles for configurations of unprotonated pocket with K^+/Cl^- with several water molecules (see Section 3.5). Table of hydration of species other than water in the absence of unprotonated pocket (Section 4.2). This material is available free of charge via the Internet at http://pubs.acs.org.

References and Notes

(1) Cahen, D.; Hodes, G. Molecules and Electronic Materials. *Adv. Mater.* **2002**, *14*, 789−798.

(2) Narayanan, R.; El-Sayed, M. A. Catalysis with Transition Metal Nanoparticles in Colloidal Solution: Nanoparticle Shape Dependence and Stability. *J. Phys. Chem. B* **2005**, *109*, 12663−12676.

(3) Cushing, B. L.; Kolesnichenko, V. L.; O'Connor, C. J. Recent Advances in the Liquid-Phase Synthesis of Inorganic Nanoparticles. *Chem. Rev.* **2004**, *104*, 3893−3946.

(4) Crooks, R. M.; Zhao, M.; Sun, L.; Chechik, V.; Yeung, L. K. Dendrimer-encapsulated Metal Nanoparticles: Synthesis, Characterization, and Applications to Catalysis. *Acc. Chem. Res.* **2001**, *34*, 181−190.

(5) Lang, H.; May, R. A.; Iversen, B. L.; Chandler, B. D. Dendrimer-Encapsulated Nanoparticle Precursors to Supported Platinum Catalysts. *J. Am. Chem. Soc.* **2003**, *125*, 14832−14836.

(6) Scott, R. W. J.; Datye, A. K.; Crooks, R. M. Bimetallic Palladium-Platinum Dendrimer-Encapsulated Catalysts. *J. Am. Chem. Soc.* **2003**, *125*, 3708−3709.

(7) Chung, Y.-M.; Rhee, H.-K. Pt-Pd bimetallic nanoparticles encapsulated in dendrimer nanoreactor. *Catal. Lett.* **2003**, *85*, 159−164.

(8) Xie, H.; Gu, Y. L.; Ploehn, H. J. Dendrimer-mediated synthesis of platinum nanoparticles: new insights from dialysis and atomic force microscopy measurements. *Nanotechnology* **2005**, *16*, S492−S501.

(9) Pellechia, P. J.; Gao, J. X.; Gu, Y. L.; Ploehn, H. J.; Murphy, C. J. Platinum ion uptake by dendrimers: An NMR and AFM study. *Inorg. Chem.* **2004**, *43*, 1421−1428.

(10) Mazzitelli, C. L.; Brodbelt, J. S. Investigation of Silver Binding to Polyamidoamine (PAMAM) Dendrimers by ESI Tandem Mass Spectrometry. *J. Am. Soc. Mass Spectrom.* **2006**, *17*, 676−684.

(11) Zhao, M.; Crooks, R. M. Dendrimer-Encapsulated Pt Nanoparticles: Synthesis, Characterization, and Applications to Catalysis. *Adv. Mater.* **1999**, *11*, 217.

(12) Grantham, L. F.; Elleman, T. S.; Martin, D. S. J. Exchange of Chlorine in Aqueous Systems Containing Chloride and Tetrachloroplatinate-(II). *J. Am. Chem. Soc.* **1955**, *77*, 2965−2971.

(13) Wu, L.; Schwederski, B. E.; Margerum, D. W. Stepwise Hydrolysis Kinetics of Tetrachloroplatinate(II) in Base. *Inorg. Chem.* **1990**, 3578−3584.

(14) Cotton, F. A.; Wilkinson, G. *Advanced Inorganic Chemistry*, 4th ed.; Wiley: New York, 1980.

(15) Tarazona-Vasquez, F.; Balbuena, P. Dendrimer-Tetrachloroplatinate Precursor Interactions. 1. Hydration of Pt(II) species and PAMAM outer pockets. *J. Phys. Chem. B* **2007**, *111*, 932−944.

(16) Diallo, M. S. Dendrimer Enhanced Ultrafiltration. 1. Recovery of Cu(II) from Aqueous Solutions Using PAMAM Dendrimers with Ethylene Diamine Core and Terminal NH2 Groups. *Environ. Sci. Technol.* **2005**, *39*, 1366−1377.

(17) Xu, Y.; Zhao, D. Revised Ion Exchange Method for Estimation of Conditional Stability Constants of Metal-Dendrimer Complexes. *Ind. Eng. Chem. Res.* **2006**, *45*, 7380−7387.

(18) Tarazona-Vasquez, F.; Balbuena, P. Complexation of Cu(II) Ions with the Lowest Generation Poly(amido-amine)-OH Dendrimers: A Molecular Simulation Study. *J. Phys. Chem. B* **2005**, *109*, 12480−12490.

(19) Cakara, D.; Kleimann, J.; Borkovec, M. Microscopic protonation equilibria of poly(amidoamine) dendrimers from macroscopic titrations. *Macromolecules* **2003**, *36*, 4201−4207.

(20) Hay, P. J.; Wadt, W. R. Ab initio effective core potentials for molecular calculations. Potentials for the transition metal atoms Sc to Hg. *J. Chem. Phys.* **1985**, *82*, 270−283.

(21) Frisch, M. J.; Trucks, G. W.; Schlegel, H. B.; Scuseria, G. E.; Robb, M. A.; Cheeseman, J. R.; Montgomery, J. A.; Vreven, T.; Kudin, K. N.; Burant, J. C.; Millam, J. M.; Iyengar, S. S.; Tomasi, J.; Barone, V.; Mennucci, B.; Cossi, M.; Scalmani, G.; Rega, N.; Petersson, G. A.; Nakatsuji, H.; Hada, M.; Ehara, M.; Toyota, K.; Fukuda, R.; Hasegawa, J.; Ishida, M.; Nakajima, T.; Honda, Y.; Kitao, O.; Nakai, H.; Klene, M.; Li, X.; Knox, J. E.; Hratchian, H. P.; Cross, J. B.; Bakken, V.; Adamo, C.; Jaramillo, J.; Gomperts, R.; Stratmann, R. E.; Yazyev, O.; Austin, A. J.; Cammi, R.; Pomelli, C.; Ochterski, J. W.; Ayala, P. Y.; Morokuma, K.; Voth, G. A.; Salvador, P.; Dannenberg, J. J.; Zakrzewski, V. G.; Dapprich, S.; Daniels, A. D.; Strain, M. C.; Farkas, O.; Malick, D. K.; Rabuck, A. D.; Raghavachari, K.; Foresman, J. B.; Ortiz, J. V.; Cui, Q.; Baboul, A. G.; Clifford, S.; Cioslowski, J.; Stefanov, B. B.; Liu, G.; Liashenko, A.; Piskorz, P.; Komaromi, I.; Martin, R. L.; Fox, D. J.; Keith, T.; Al-Laham, M. A.; Peng, C. Y.; Nanayakkara, A.; Challacombe, M.; Gill, P. M. W.; Johnson, B.; Chen, W.; Wong, M. W.; Gonzalez, C.; Pople, J. A. *Gaussian 03*, revision C.02; Gaussian, Inc.: Wallingford, CT, 2004.

(22) Balogh, L.; Tomalia, D. A.; Hagnauer, G. L. A revolution of nanoscale proportions. *Chem. Innovation* **2000**, *30*, 19−26.

(23) Ohtaki, H.; Radnai, T. Structure and Dynamics of Hydrated Ions. *Chem. Rev.* **1993**, *93*, 1157−1204.

(24) Harding, M. M. Metal-ligand geometry relevant to proteins and in proteins: sodium and potassium. *Acta. Crystallogr.* **2002**, 872−874.

(25) Marcus, Y. Thermodynamics of Solvation of Ions. Part 5.- Gibbs Free Energy of Hydration at 298.15 K. *J. Chem. Soc. Far. Trans.* **1991**, *87*, 2995−2999.